Tensile fracture morphologies of bulk metallic glass

R. T. Qu,[1] M. Stoica,[2] J. Eckert,[2,3] and Z. F. Zhang[1,a)]
[1]*Shenyang National Laboratory for Materials Science, Institute of Metal Research, Chinese Academy of Sciences, 72 Wenhua Road, Shenyang 110016, People's Republic of China*
[2]*Institute for Complex Materials, IFW Dresden, P.O. Box 270016, D-01171 Dresden, Germany*
[3]*Institute of Materials Science, TU Dresden, D-01062 Dresden, Germany*

(Received 23 May 2010; accepted 9 August 2010; published online 17 September 2010)

The fracture morphology plays a much important role not only for the failure analysis of materials but also for the clarification of their fracture mechanisms. However, quantitative analysis of the fracture morphology of bulk metallic glasses (BMGs) is still very lacking. In this study, both model and mechanical experiments were conducted to reveal the development of the fracture morphology and the effect of stress state. Inclined notch tensile specimens of a Zr-based BMG with different notch angles were designed to obtain various stress states. For the first time, some new parameters to describe the tensile fracture surfaces of the BMG specimens were proposed. Statistical analysis of these parameters shows that the stress state has a significant influence on the features of fracture surfaces. Through a discussion on the structure and heat evolution during tensile deformation, two damage mechanisms associated with thermal softening and weakening by defects are found to have a combined effect on the tensile fracture of BMG. © *2010 American Institute of Physics*. [doi:10.1063/1.3487968]

I. INTRODUCTION

In the last two decades, varieties of bulk metallic glasses (BMGs) have been synthesized and extensively investigated.[1–3] Due to the shear localization of plastic deformation at room temperature, BMGs often show brittle fracture behavior.[4–6] In order to improve the mechanical performance, plenty of researches have been focused on the behaviors of shear bands, methods to improve toughness and the synthesis of new BMGs.[3,5] However, concerning the fracture morphologies of BMGs, little progress has been made except for the nanoscale configurations observed in some brittle BMGs[7–10] or under dynamic loading.[11,12] Systematic and detailed research on the quantitative analysis of fracture surfaces is very limited. For conventional metallic materials, the analysis of fracture morphologies plays a very important role in the failure analysis and safety design of the engineering components.[13] For BMG materials, due to their extremely high strength and their special fracture features, studies on the fracture surfaces are of significance not only for engineering applications, but also for the clarification of the basic fracture mechanisms.

The most extensive research on the fracture morphologies of metallic glasses was done in 1970s.[14–20] For example, Leamy *et al.*[14] were the first to report the microscopic features observed on the tensile fracture surfaces of some Pd-based glassy ribbons. They divided the fracture surface into two distinct regions: a smooth region and a vein pattern. The smooth region was attributed to the plastically shear deformation prior to fracture, while the vein pattern resulted from local heating and viscous flow necking of material between propagating cracks or voids.[14] Later, Spaepen and Turnbull[16] calculated the free volume increment due to the existing hydrostatic tension at the head of a crack in a ribbon pulled in tension, and found that the increased free volume lowered the viscosity within that region down to typical values of fluids. Hence, they thought that the vein pattern was formed by separating a fluid layer between two solid surfaces. Pampillo and Reimschuessel[15,17] proposed that the concentrated shear deformation prior to failure defines a weaker "pseudocleavage" plane on which nucleation and propagation of cracks would occur with greatest ease. Pseudocleavage propagates from the nucleation site until it meets other growing cracks, defining a pseudocleavage zone surrounded by a main vein.

It is worth noting that the features obtained by model experiment of separating two glassy slides within a viscous medium closely resemble the veins on the fracture surface of metallic glasses.[15,17,19] The formation of the characteristic features is attributed to the Taylor instability[21] which occurs at the moving boundary between two immiscible fluids in the case of air and the viscous medium. The resemblance strongly supports that the vein pattern was formed by separating a fluid layer between two solid surfaces as proposed by Spaepen and Turnbull.[16] Vein patterns have been extensively observed not only in tension but also in compression where the hydrostatic stress or normal stress acting on the shear band is negative.[22,23] This indicates that the fluid layer should not only depend on the hydrostatic tension. Recently, the generation of heat because of shear deformation within a shear band has been extensively studied.[24–27] For example, local melting and an intensive temperature rise were observed for various BMGs under deformation.[25,26] Therefore, the fluid layer may originate from two sources: hydrostatic tension and local heating by shear deformation.

Based on the assumption that the veins formed by separating a fluid layer between two solid surfaces, Argon and Salama[20] used the logarithmic spiral slip line field theory and

a)Electronic mail: zhfzhang@imr.ac.cn.

Spaepen[18] used the perturbation theory to explore the physical reason behind the vein pattern. They achieved relationships between the dimensions of the features and mechanical properties, providing some methods to develop it into a failure analysis by analyzing the details of the vein patterns on the fracture surface. However, the proposed models still need further experimental examination and verification.

The above mentioned investigations on the fracture morphologies concerned mainly the tensile failure of metallic glassy ribbon. For BMG samples with large size, loading modes besides tension (e.g., compression) can be conducted and some interesting features have been observed. For instance, careful observations on the fracture morphologies formed under compression show much different from those formed under tension.[22] Although smooth regions can be found in both cases, patterns with only uniform shear veins were observed on the compressive fracture surface, while radiating veins together with smooth cores were found on tensile fracture surfaces.[22] The only one difference in the stress states between compression and tension is the normal stress acting on the fracture plane, which is positive for tension but negative for compression. Hence, the stress state must play an important role in the development of fracture morphologies and needs further study.

For BMGs under tension, the specimen often fails along a single shear plane. The resolved normal stress σ and the shear stress τ on planes with different angles θ can be expressed as,[22]

$$\tau = \sigma_A \sin\theta \cos\theta, \tag{1a}$$

$$\sigma = \sigma_A \sin\theta \sin\theta, \tag{1b}$$

where σ_A is the applied stress. This demonstrates that by controlling the fracture along different shear planes, various stress states with different combinations (σ, τ) of normal and shear stresses at the moment of fracture can be obtained according to Eq. (1).

The aim of this work is to study the tensile fracture mechanism of BMGs through a quantitative analysis of fracture morphologies of samples with different stress states. In order to obtain a series of stress states (σ, τ), inclined notch tensile BMG specimens with different notch angles were designed. The inclined notches reduce the net loading area and thus induce fracture along the notch plane. After fracture, a high-resolution scanning electron microscope (SEM) was used to observe the tensile fracture surfaces carefully. Besides the mechanical experiments, model experiment was also conducted to uncover the formation of the fracture morphologies. For the first time, new parameters that describe the differences in the tensile fracture morphologies of BMGs are proposed. Statistical analysis of these parameters shows that the stress state has a significant influence on the features of the fracture surfaces. Through an analysis of the structure and heat evolution during tensile deformation, it is proposed that the heat and defects may be two controlling factors for the tensile failure of BMGs.

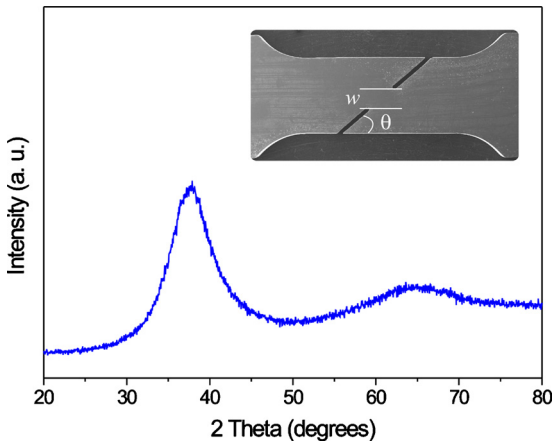

FIG. 1. (Color online) XRD pattern of the studied BMG. The inset shows a part of a typical inclined notch tensile specimen with a notch angle of 40°.

II. EXPERIMENTAL METHODS

$Zr_{52.5}Cu_{17.9}Ni_{14.6}Al_{10}Ti_5$ BMG plates with dimensions of $40 \times 30 \times 1.8$ mm^3 were prepared by copper mold casting in a high-purity argon atmosphere. The amorphous structure of the specimens was identified by standard x-ray diffraction (XRD), as shown in Fig. 1. Tensile specimens with gauge dimensions of $6 \times 3 \times 1.5$ mm^3 were cut from the BMG plates by an electric spark cutting machine and were subsequently ground and polished by 2.5 μm abrasive paste.

Inclined notch tensile specimens were prepared by cutting notches into the above polished tensile specimens by electric spark cutting, which created a notch width of ~0.2 mm and a notch radius of ~0.1 mm. A typical 40° sample is shown in the inset of Fig. 1. The effective width (w), the notch angle (θ), and the thickness (B) were measured by Leo Supra 35 high-resolution SEM and microcallipers. For simplicity, all the notched specimens were labeled with their notch angles. The tensile specimens with or without notches were tested using an MTS 810 testing machine at a constant strain rate of about 10^{-4} s^{-1} at room temperature in air. The fracture morphologies of all samples were observed with the Leo Supra 35 high-resolution SEM.

The model experimental test was conducted by separation of slides of window glass coated with a viscous material.[19] The viscous material, which was a mixture of shampoo and ink, was distributed homogenously between two glassy slides, as shown in Fig. 2(a). Two ways of separation were used. As illustrated in Fig. 2(b), the separation mode A subjects the viscous material to both a shear force and a normal force. In case of separation mode B, the slides were opened with only a normal force at one side of the slides [see Fig. 2(c)].

III. RESULTS

A. Model experiment of the separation of a fluid

The results of the two separation modes A and B are shown in Figs. 2(d) and 2(e), respectively. A vein pattern together with a smooth region [see Fig. 2(d)], which is similar to the typical fracture morphologies of metallic glasses, was obtained in case of separation mode A with inclined

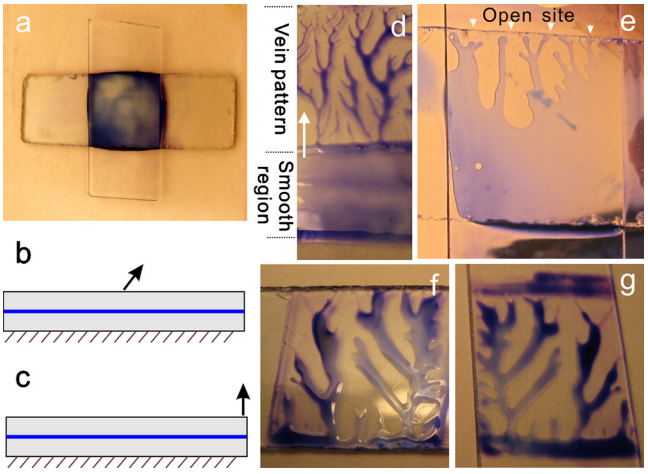

FIG. 2. (Color online) Photos of the devices (a) and the resulting patterns (d)–(g) of the model experiment and [(b) and (c)] illustrations of the method to separate the two window glass slides.

driven force. This similarity demonstrates that the formation of the fracture morphologies of BMGs is a result of separating two slides of solid material with a viscous layer in between.

Opening slides at one side (mode B) create veins with ridges always pointing toward the open site, as indicated in Fig. 2(e). The reason for this phenomenon is that the open site is the initial position where the second fluid (air, in this case) starts to enter into the first one (viscous materials) by the Taylor instability.[21] This phenomenon is important because in light of this we can explore the initial formation sites of veins by examining the open sites of the vein pattern. The morphologies of two opposing separated slides are shown in Figs. 2(f) and 2(g), where the one-to-one correspondence is obvious for the two patterns.

B. Tension of samples with and without notches

The unnotched tensile sample failed at a stress of about 1660 MPa with a shear fracture angle of 50.74° with respect to the loading axis.[28] Obviously, the shear fracture angle deviates from 45° corresponding to the maximum shear stress plane, indicating a normal stress effect on the fracture behavior.[28] According to Eq. (1), the normal and shear stresses acting on the fracture plane at the moment of fracture are 995 MPa and 813 MPa, respectively.

By measuring the fracture stresses of the notched samples with different notch angles, various stress states with different combinations (σ, τ) of normal and shear stresses at the moment of fracture were obtained according to Eq. (1). The shear and normal stresses on the fracture plane of notched samples are plotted in Fig. 3, revealing that the failure of the BMG samples follows the Ellipse criterion.[28,29] The results indicate that as the notch angle increases, the shear stress on the fracture plane decreases, while the normal stress increases. This variation in the stress state in a large range provides a good method to explore the stress state effect on the tensile fracture morphology of metallic glasses, which will be discussed in the following sections.

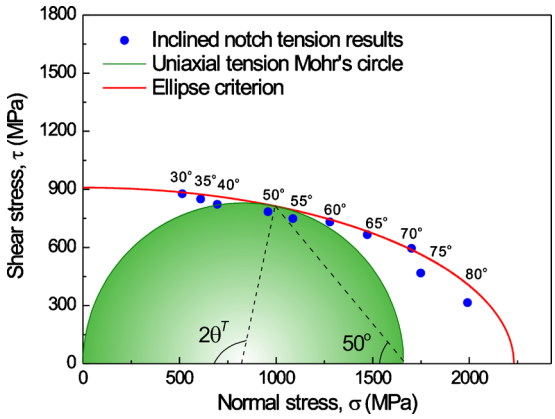

FIG. 3. (Color online) Variation in the shear fracture stress with the normal stress acting on the shear plane (Ref. 28). The critical fracture lines of the Ellipse criterion as well as the uniaxial tension Mohr's circle are plotted for comparison.

C. SEM observations

1. Tensile fracture morphologies of unnotched samples

The unnotched samples display typical features of veins and smooth regions,[14,22] as shown in Figs. 4(a) and 4(b). The fracture surface observations demonstrate that the features have a good one-to-one relationship on the two opposing fracture surfaces in identical samples, as shown in Figs. 4(c) and 4(d), which is similar to the results of the model experiment displayed in Fig. 2. This gives further evidence for the inference that the fracture patterns of BMGs originate from the separation of a viscous fluid.

Careful comparison demonstrates that there is still a certain difference in the vein patterns between the truly fractured surface [see Fig. 4(a)] and that obtained by model experiment [see Fig. 2(d)]. For the vein pattern on the tensile fracture surface, the ridges of the veins are radiating and point toward a smooth core, as indicated by the arrows in Fig. 4(a). The radiating ridges with smooth core become the characteristic features of the vein pattern. In contrast, all the ridges are branchlike and point to the same direction, i.e., the

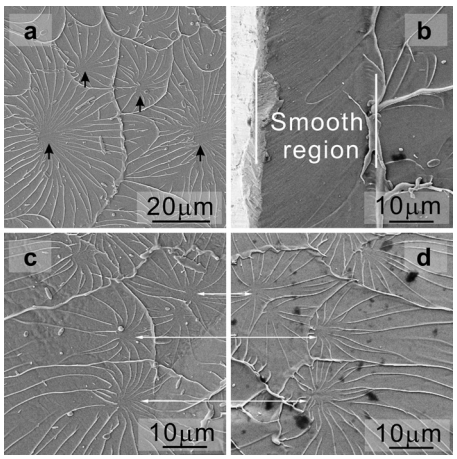

FIG. 4. Fracture morphologies of the unnotched tensile sample. (a) Vein patterns of radiating ridges and smooth cores (black arrows); (b) smooth regions; (c) and (d) are the corresponding images from two opposing fracture surfaces.

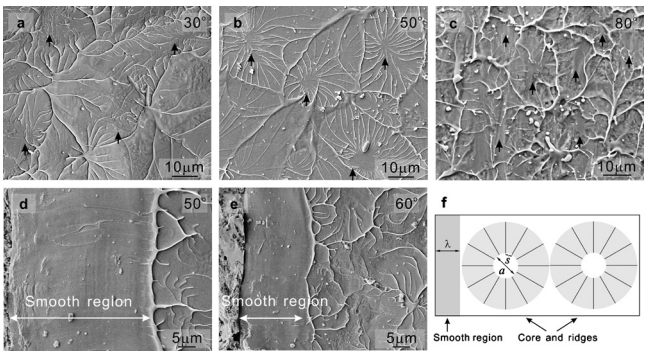

FIG. 5. Fracture morphologies of typical inclined notch tensile samples. [(a)–(c)] The vein patterns of samples with notch angle 30°, 50°, and 80°. The black arrows show the sites where the ridges of the veins point to. [(d) and (e)] The smooth regions of samples 50° and 60°. (e) Illustration of tensile fracture morphology.

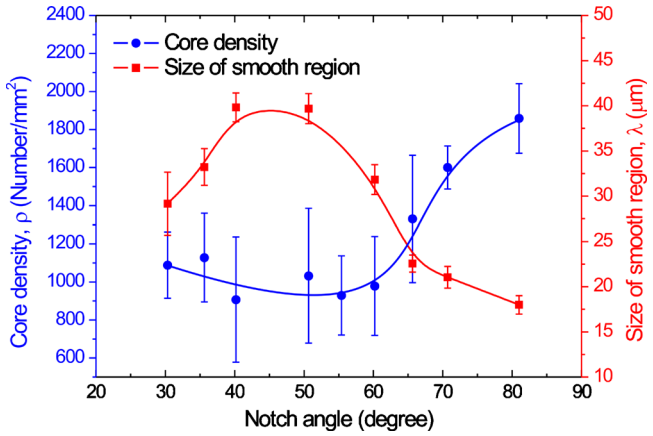

FIG. 6. (Color online) Statistical results of the size of the smooth region λ and the core density ρ of samples with different notch angles.

open site, for the vein pattern obtained by model experiment [see Figs. 2(d) and 2(e)]. Because of the similar physical reason for the formation of two kinds of vein patterns (the Taylor instability), it can be deduced that the smooth cores on the tensile fracture surface should be the initial open sites of the sample prior to final fracture. Leamy *et al.*[14] claimed that the cores should be the origin of crack. Pampilo and Reimschuessel[15] observed some hard undeformed impurities in the cores and argued that the crack initially formed from these impurities. In fact, our careful observations on plenty of cores on tensile fracture surfaces show that only few impurities can be found. Our previous work has shown that there are many microcracks within shear bands prior to fracture.[30,31] Although those microcracks are hard to be captured in the samples under unconstrained tension, they can be easily found in samples after the confined loadings, like rolling,[32] bending,[31] small punch test,[30] and compression.[33] Recently, when we observed shear bands in samples before compressive fracture, many microcracks with sizes in the range of 1–6 μm were found in various BMGs.[33] Therefore, the cores on the tensile fracture surface should correspond to the microcracks within shear bands at the moment of fracture.

2. Tensile fracture morphologies of notched samples

The tensile fracture surfaces of the samples with inclined notch also consist of two regions: a smooth region and the vein pattern (Fig. 5). The vein pattern is obviously different for samples with different notch angles [Figs. 5(a)–5(c)]. The characteristic features of radiating ridges with smooth cores for unnotched tensile sample are only apparent for the sample with a notch angle of 50° [Fig. 5(c)]. This similarity of the fracture morphologies is consistent with the approximation of stress states because the unnotched sample failed at an angle of 50.74°. This indicates that the vein patterns on the tensile fracture surfaces are controlled by the stress state, i.e., shear and normal stresses, which will be further discussed later.

In order to look for some clues to describe the irregular vein patterns of the inclined notch samples, the sites where the ridges point to were explored, because the results of the model experiment indicate that the ridges of vein pattern often point to the open site. Surprisingly, although the vein patterns are obviously different, the ridges of all veins initially start from relatively smooth cores, as indicated by the arrows in Figs. 5(a)–5(c). This is similar to the unnotched tensile sample [see Fig. 4(a)], although the core may not be as perfectly circular. Hence, it is reasonable to consider that the "core and ridges" should be the basic elements of the vein pattern for the tensile fracture morphology of BMG. Incorporating the smooth region, the whole fracture morphology of a tensile sample with or without notches can be schematically described as in Fig. 5(f).

First, the smooth region is often regarded as a result of stable plastic shearing and should be the critical shear offset of BMGs.[14,30,31] By measuring the size of the smooth region, the plastic displacement can be estimated, providing data to calculate the work of deformation. Second, similar to the above observed features of the unnotched tensile sample [see Fig. 4(a)], the observed cores should also be related to the microcracks within shear bands prior to fracture. These microcracks can be regarded as the result of materials damage after deformation. Detailed investigations on the microcracks (here cores on the fracture surfaces) may shed light on the tensile deformation and damaging mechanisms of BMGs. Therefore, to describe the vein pattern on the tensile fracture surface, four parameters may be considered: the size of the smooth region (λ), the core density (ρ), the mean size of cores (a), and the spacing between ridge tips (s), as displayed in Fig. 5(f). In Sec. III D, we will present the statistical results on the variation in these parameters with samples failed at different stress states.

D. Statistical results

Figure 6 shows the statistical results of the core density (ρ) and the size of the smooth region (λ) varying with notch angles. First, the two parameters ρ and λ are not constant for all the samples with various notch angles. Rather, the size of the smooth region (λ) reaches a peak value at notch angles of 40–50°; while as notch angle increasing, the core density (ρ) decreases slightly for notch angles below 55°, and then increases significantly. Considering the experimental errors and the uniqueness of the 50° notched sample, which pos-

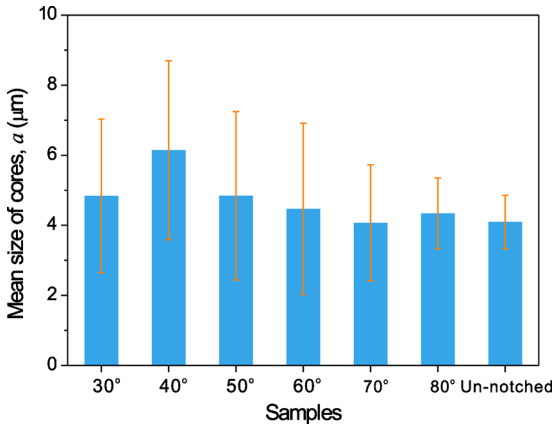

FIG. 7. (Color online) Statistical results of the mean size of cores a for samples with or without notches.

sesses the most alike fracture morphology and the approximately same shear fracture angle as the unnotched sample, the statistical results presented in Fig. 6 demonstrate that the 50° notched sample should possess the widest smooth region and the minimum core density. As indicated in the above sections, the smooth region represents the critical shear offset prior to fracture and the core density stands for the amount of microcracks in the primary shear bands. This means that for the BMG samples with different notch angles, the 50° notched sample has the maximum shear offset but the minimum amount of microcracks at the moment of fracture.

The statistical distribution of the mean size of cores (a) for the different BMG samples is presented in Fig. 7. Although a large scatter exists, the data indicate that the core size is around 5 μm, which is consistent with the previous results on the same alloy.[31] The approximately same mean core size represents the similar critical length of the microcracks for different BMG samples. Our previous observations on BMG samples with a similar composition after small punch test also showed a critical length of microcracks of ~5 μm.[30] These results imply that the critical size of microcracks (or cores) may be independent on the stress state and can be treated as an intrinsic critical condition for subsequent catastrophic fracture.

The statistical distribution of the spacing between ridge tips (s) for different samples is presented in Figs. 8(a)–8(d). Obviously, the samples with notch angles of 30° and 70° exhibit a more scattered distribution of s, while the distributions for 50° and unnotched samples are similar and rather narrow. The average spacings of the different samples are plotted in Fig. 8(e). The 50° and unnotched samples have a spacing of ~0.5 μm, while the spacings of the 30° and 70° samples are larger. For the spacing between ridge tips s, Argon and Salama[20] derived an equation

$$s = 12\pi^2 A(n)\left(\frac{\chi}{\tau}\right), \tag{2}$$

where χ is the surface stress, τ is the shear stress, and $A(n)$ is a wavelength coefficient. For the present samples with the same composition and fabrication conditions, χ and $A(n)$ are constants. Hence, according to Eq. (2), the product $\tau \times s$ of the spacing s between ridge tips and the shear stress τ should

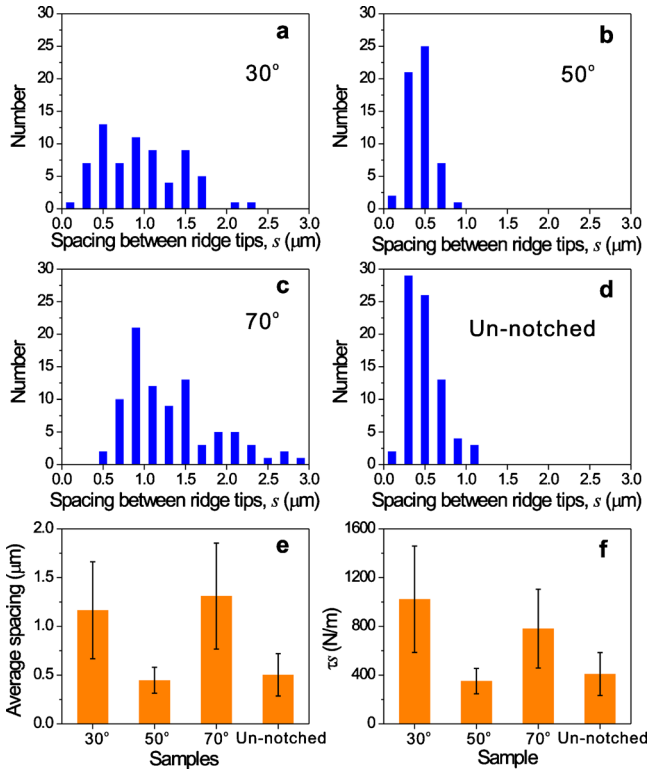

FIG. 8. (Color online) Statistical distributions of the spacing between ridge tips s of (a) 30°, (b) 50°, and (c) 70° notched sample and (d) unnotched sample. (e) The average spacing of different samples. (f) The values of τs of different samples.

be constant. However, the statistical results of $\tau \times s$ are not uniform for different samples [Fig. 8(f)]. The value $\tau \times s$ of the 50° sample is approximately the same as that for the unnotched sample but is the minimum one among all the inclined notch samples. This is inconsistent with Eq. (2). Different notch angles induce different stress states because both the normal and shear stresses vary with notch angles (see Fig. 3). However, in the theory of Argon and Salama,[20] only the shear stress was considered. The present results show that the normal stress may influence the spacing between ridge tips remarkably and should not be neglected. Therefore, the tensile fracture morphologies and mechanisms of BMGs should be controlled by both shear and normal stresses and will be further discussed in details as below.

IV. DISCUSSION

The above described results reveal that the stress state has a significant influence on the tensile fracture morphologies of BMGs. With varying the notch angles of the tensile specimens, both the shear stress and normal stress on the fracture plane change monotonically. However, the characteristic features of the tensile fracture morphologies do not show a monotonic variation, as shown in Figs. 6–8. This demonstrates that both the shear stress and normal stress play important roles in the tensile deformation and fracture behaviors of BMGs. In the following sections, first, the effects of shear stress and normal stress on the tensile fracture mechanisms of BMGs will be discussed in more details, re-

spectively. Based on these discussions, the processes of tensile failure and the formation mechanisms of the fracture morphologies are then presented.

A. Effect of shear stress on tensile fracture behaviors

When a BMG sample is subjected to a high load, some changes in structure may happen. Cheng *et al.*[34,35] found that the full-icosahedral clusters, which are more chemically and kinetically stable, should be key local structural motif that constitutes the main resistance for the plastic flow to commence in the Cu–Zr metallic glasses. On the other hand, it is well agreed that the free volume also plays important role in the deformation and fracture of BMGs.[5,36,37] The free volume increases upon deformation and decreases upon relaxation.[36] According to the theory of Spaepen and Steif,[36,38] the steady state free volume is positively related to the applied shear stress τ, that is, the larger τ, the more steady state free volume v_f. In addition, the excess free volume produced by plastic deformation can induce dilatation of materials.[39–41] The fact that BMGs have a lower density after severe plastic deformation like rolling[39] is a strong evidence for dilatation.

In addition, it is accepted that the free volume produced by plastic deformation is unstable. Through thermodynamic calculations, Wright *et al.*[42] found that the free volume is prone to coalescence and nanoscale voids can form spontaneously. Donovan and Stobbs,[43] reported the existence of nanoscale voids as revealed by an enhanced small-angle scattering signal in shear bands. Li *et al.*[44] developed a method to quantitatively analyze the high-resolution transmission electron microscopy (TEM) image to identify and characterize nanoscale defects in metallic glasses. By using this method, Li *et al.*[44] and later Jiang and Atzmon[45] observed a high concentration of nanoscale voids in shear bands of metallic glasses.

During the process of plastic deformation, besides the change in structure, the generation of heat should also be considered. According to Lewandowski and Greer,[25] a dramatic temperature rise occurs during shear deformation of metallic glass. The heat is essentially induced by the release of elastic energy, and should be associated with the shear plastic work, which takes place mostly in the primary shear band driven by a shear stress τ and a total displacement λ (the critical shear offset, i.e., the size of the smooth region[31,46]). Assuming the efficiency of heat-work transformation as β, following Zhang *et al.*,[26] the heat content can be written as,

$$H = \beta\tau\lambda = \beta H_R, \tag{3}$$

where $H_R \equiv \tau\lambda$ is the relative heat content, also standing for the sum of introduced mechanical work.

Besides the generation of heat, the release of heat takes place at the same time, but is proportional to the time of shearing,[47] and thus the heat accumulates.[30] Experiments have demonstrated that the heat affected zones are becoming wider,[26,27] and the viscosity of shearing materials decreases,[30] as shear deformation proceeds along shear band. Hence, assuming that the duration of shear (total time of plastic deformation) for the present notched and unnotched samples are the same, a larger H_R should correspond to more accumulated heat prior to fracture. Therefore, the shear stress τ has an important positive effect on both the increment of free volume and the generation of heat.

B. Effect of normal stress on tensile fracture behaviors

Based on the free volume model, Flores and Dauskardt[48] proposed that the mean stress σ_m mainly influences the initial free volume v_i, i.e.,

$$v_i = v_0 + \Omega\frac{\sigma_m}{B}, \tag{4}$$

where v_0 is the initial free volume without superimposed mean stress, Ω is the atomic volume, and B is the bulk modulus. Under tensile loading, the local mean stress is positive and can thus substantially increase the initial free volume dramatically.

Considering the local stress field around a mature shear band in a sample under uniaxial tension, the applied tensile stress σ_A can be resolved into two parts: normal stress σ and shear stress τ according to Eq. (1). If we neglect the stress concentration induced by the local softening in shear band, the mean stress σ_m can be written as: $\sigma_m = \sigma_A/3 = \sigma/(3\sin^2\theta)$, where θ is the shear band angle. Hence, in view of free volume, the normal stress σ mainly increases the initial free volume v_i [Eq. 4]. Calculations by Steif and Spapen[38] have shown that a small increment of the initial free volume will dramatically increase the excess free volume and thus increase the volume fraction of voids and dilatation. The calculations by Wright *et al.*[42] and the TEM observations by Jiang and Atzmon[45] proved this trend of normal stress effect. They found that the volume fraction of voids in glassy alloys deformed in tension is much larger than that in compression, providing further evidence for the significant effect of normal stress on the production of defects.

C. Tensile failure mechanisms of BMGs

The above analysis of the stress state effect shows that two aspects may be the major issues during plastic deformation of metallic glasses: the generation of heat and the change in local structure. As discussed above, the heat is produced by shear plastic work and can be accumulated with continuous shearing, inducing a temperature rise and causing local softening of the materials.[25,26] Thus, the "thermal softening" should be one of the reasons for the damage of shear band in metallic glasses. On the other hand, with shearing proceeding within localized shear band, the free volume increases and thus defects (like voids) accumulate and grow.[42,45] When large adjacent voids link with each other, microcracks will form. Because the stress concentrations existing in the front of the tip of microcracks can locally weaken the materials, the development of defects should be another reason for the damage of shear band in metallic glasses.

To further uncover the connections between thermal softening and the development of defect, the two aspects

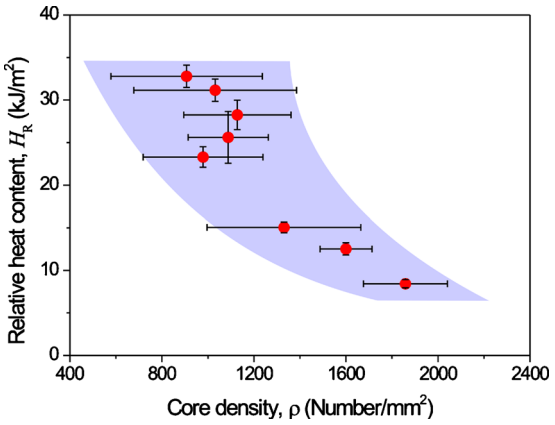

FIG. 9. (Color online) Plot of data of the relative heat content H_R and the core density ρ.

responsible for the failure of BMGs, we plot the relative heat content H_R versus the core density ρ as shown in Fig. 9, because H_R and ρ can represent the amount of heat and defects to some extent. An inverse relationship between H_R and ρ is obvious. When more heat is produced by shear deformation, the fracture can happen at a relatively lower density of cores or microcracks. In the opposite case, i.e., when the defects within the local shear band are abundant, it is not necessary to impose much mechanical work or to produce a large amount of heat to break the specimen. This means that the failure of BMG is controlled by the *combined damage effect* of heat and defects, not only by one of them.

According to the above analysis, the tensile failure processes of a BMG sample can be illustrated as Fig. 10. Once the stress conditions for yielding are satisfied, plastic deformation occurs. At room temperature, the plastic deformation of BMG always localizes into a very narrow shear band.[5] Despite the reason for the formation of shear band may not be widely understood, recent studies show that the thermal softening is not a cause of the initial shear localization.[25,35] Further, molecular dynamics simulation by Cao *et al.*[35] in Cu–Zr BMG shows a loss of the stable full-icosahedral clusters when shear banding happens and thus the structural softening may be responsible for the shear band initiation.

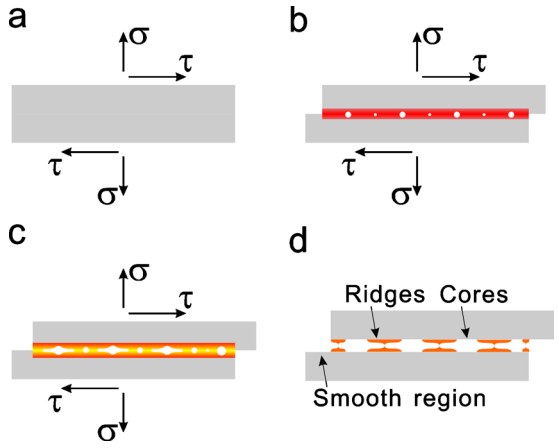

FIG. 10. (Color online) Illustration of the evolution of heat and local structure in a shear band under tensile loading.

Once shear band penetrates across the entire sample, shear offset will be observed as steps on the external surfaces of sample [see Fig. 4(b) and 5(d)], and as illustrated in Fig. 10(b). Owing to the structural softening inside the already formed shear band, further deformation will mainly localize in this band. As shearing proceeds, the shear offset increases gradually;[30] and accordingly, the local structure inside the shear band will be further changed. The excess free volume increases and coalesces to form voids; meanwhile, heat can also be generated by plastically shear deformation, as illustrated in Fig. 10(b). As the plastic deformation continues and the shear offset increases, more heat will be accumulated and the voids will coarsen. By linkage of the coarsened voids, microcracks can be formed[30,31] [see Fig. 10(c)]. It should be noted that there may be some structural inhomogenities which are introduced during the casting process of the sample.[49,50] The inhomogeneities can promote or prevent the initiation and propagation of shear band and crack, depending on their length scale and distribution.[49,50] Nevertheless, during the shearing process, the local material in shear band has been damaged by both thermal softening and development of defects, leading to the reduction in the load bearing capability continuously. As shearing deformation proceeds, when a critical state is reached, the local material in shear band will fail to bear the applied load and sample will fracture along the shear band, as shown in Fig. 10(d). As results of the shear offset, the temperature rise and the microcracks within the shear band, the smooth region and the vein pattern consisting of the core and ridges are formed on the final fracture surface, as the observations in Fig. 5.

Altogether, the above discussions demonstrate that the tensile failure of BMGs is controlled by local heating and the structural evolution during plastically shear deformation. The critical state for tensile fracture is a combined result of thermal softening and development of defects. The stresses acting on the shear plane provide the driving force for local heating and the generation of defects. Both the tensile normal stress and the shear stress have the capability to increase the free volume and further to increase the amount of voids or even microcracks. In addition, the mechanical work driven by the shear stress is responsible for the generation of heat and thus the thermal softening. By changing the stress states on the shear plane, the ratio of contribution of heat and defects on damaging of the BMGs is changed and the observed final fracture morphologies are also different. As summarized in Fig. 11, when the stress state on the fracture plane approaches to that of the intrinsic fracture plane of smooth specimen (i.e., 50° plane for present Zr-based BMG), the accumulated heat increases but the defects decreases. This finally leads to a morphology with the maximum smooth region and the minimum core density in comparison with those fracturing along planes with other stress states. On the other hand, with stress states departing from that of the intrinsic fracture plane, the weakening by defects becomes the dominating reason for the tensile failure of the samples rather than the thermal softening, and tensile fracture morphologies with high core density are formed.

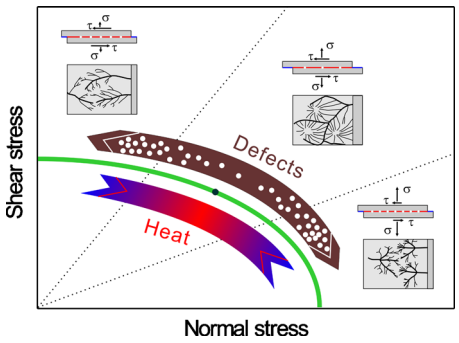

FIG. 11. (Color online) Summary of the stress state effect on the tensile fracture morphologies and the damage mechanisms. The solid curve represents the critical fracture stress line, which should be an ellipse as proved in Ref. 28. The black dot at the curve stands for the stress state of the intrinsic fracture plane (i.e., 50° plane).

V. CONCLUSIONS AND REMARKS

The tensile fracture processes and mechanisms of BMG samples with different notch angles have been discussed in comparison with a model experiment by separating two window glass slides. It is found that the typical morphology of vein pattern together with smooth region is the result of splitting two solid surfaces with a layer of viscous material in between by an inclined force. The model experiment also reveals that the ridges of the veins point to the open sites. This makes it possible to seek for the initial microcracks prior to fracture by the investigation on the fracture surfaces of BMG. Furthermore, through studying the tensile fracture morphologies, four parameters are proposed to describe the fracture features by considering the stress state effect, i.e., the size of the smooth region, the density of cores, the mean size of cores, and the spacing between the ridge tips of veins.

Statistical analysis of the fracture morphologies of inclined notch tensile samples reveals a significant effect of the stress state. The results demonstrate that both the shear stress and normal stress play important roles in the tensile deformation and fracture behavior of BMGs. Further discussions on the effects of shear stress and normal stress on the fracture behaviors indicate that two factors of heat and defects should be the controlling factors for tensile fracture. For samples with different stress states, the damage of materials is a result of the combined effect of heat and defects.

When BMG yields under tensile loading, plastic deformation occurs in a major shear band. As the shear offset increases, the heat accumulates while structural defects develop and finally evolve into microcracks. Both heat accumulation and the development of defects damage the material. When a critical condition is satisfied, the specimen breaks and fracture morphologies form. The characteristic features observed on the fracture surface are traces of the local structure of the shear band before fracture and provide abundant information about the deformation and fracture of BMGs. The smooth region observed on the fracture surface correlates with the shear offset at the moment of fracture, i.e., the critical shear offset. The cores of the veins are microcracks existing in the shear band prior to fracture. And the spacing between the ridge tips of veins can be regarded as a representation of some mechanical properties of the material, like the fracture toughness.[20]

The fracture morphologies formed at the moment of fracture provide many clues to explore the deformation and fracture mechanisms of materials. The present work is our first attempt to uncover the implied fracture mechanisms by the observations of fracture surfaces under different stress states. The methods proposed here to describe the fracture features may be helpful not only for a better understanding of the fracture mechanisms of BMGs but also for the failure analysis of BMG components.

ACKNOWLEDGMENTS

RTQ thanks Dr. K. Wang for the experimental assistance. This work was financially supported by the National Natural Science Foundation of China (NSFC) under Grant Nos. 50401019, 50871117, 50890173 and the National Basic Research Program of China under Grant No. 2010CB631006. One of the authors (Z. F. Zhang) also wishes to acknowledge the National Outstanding Young Scientist Foundation under Grant No. 50625103 and the Alexander von Humboldt (AvH) Foundation for financial support and the China/Germany Joint Research Programme (PPP) for financial support.

[1] W. L. Johnson, MRS Bull. **24**, 42 (1999).
[2] A. Inoue, Acta Mater. **48**, 279 (2000).
[3] W. H. Wang, C. Dong, and C. H. Shek, Mater. Sci. Eng. R **44**, 45 (2004).
[4] M. F. Ashby and A. L. Greer, Scr. Mater. **54**, 321 (2006).
[5] C. A. Schuh, T. C. Hufnagel, and U. Ramamurty, Acta Mater. **55**, 4067 (2007).
[6] Z. F. Zhang, F. F. Wu, G. He, and J. Eckert, J. Mater. Sci. Technol. **23**, 747 (2007).
[7] X. K. Xi, D. Q. Zhao, M. X. Pan, W. H. Wang, Y. Wu, and J. J. Lewandowski, Phys. Rev. Lett. **94**, 125510 (2005).
[8] Z. F. Zhang, F. F. Wu, W. Gao, J. Tan, Z. G. Wang, M. Stoica, J. Das, J. Eckert, B. L. Shen, and A. Inoue, Appl. Phys. Lett. **89**, 251917 (2006).
[9] G. Wang, D. Q. Zhao, H. Y. Bai, M. X. Pan, A. L. Xia, B. S. Han, X. K. Xi, Y. Wu, and W. H. Wang, Phys. Rev. Lett. **98**, 235501 (2007).
[10] J. Shen, W. Z. Liang, and J. F. Sun, Appl. Phys. Lett. **89**, 121908 (2006).
[11] M. Q. Jiang, Z. Ling, J. X. Meng, and L. H. Dai, Philos. Mag. **88**, 407 (2008).
[12] J. X. Meng, Z. Ling, M. Q. Jiang, H. S. Zhang, and L. H. Dai, Appl. Phys. Lett. **92**, 171909 (2008).
[13] J. Rösler, H. Harders, and M. Bäker, *Mechanical Behaviour of Engineering Materials* (Springer-Verlag, Berlin, 2007).
[14] H. Leamy, T. Wang, and H. Chen, Metall. Mater. Trans. B **3**, 699 (1972).
[15] C. A. Pampillo and A. C. Reimschuessel, J. Mater. Sci. **9**, 718 (1974).
[16] F. Spaepen and D. Turnbull, Scr. Metall. **8**, 563 (1974).
[17] C. A. Pampillo, J. Mater. Sci. **10**, 1194 (1975).
[18] F. Spaepen, Acta Metall. **23**, 615 (1975).
[19] S. Takayama and R. Maddin, Philos. Mag. **32**, 457 (1975).
[20] A. S. Argon and M. Salama, Mater. Sci. Eng. **23**, 219 (1976).
[21] P. G. Saffman and G. Taylor, Proc. R. Soc. London, Ser. A **245**, 312 (1958).
[22] Z. F. Zhang, J. Eckert, and L. Schultz, Acta Mater. **51**, 1167 (2003).
[23] Z. F. Zhang, G. He, J. Eckert, and L. Schultz, Phys. Rev. Lett. **91**, 045505 (2003).
[24] W. J. Wright, R. B. Schwarz, and W. D. Nix, Mater. Sci. Eng., A **319–321**, 229 (2001).
[25] J. J. Lewandowski and A. L. Greer, Nature Mater. **5**, 15 (2006).
[26] Y. Zhang, N. A. Stelmashenko, Z. H. Barber, W. H. Wang, J. J. Lewandowski, and A. L. Greer, J. Mater. Res. **22**, 419 (2007).
[27] H. Guo, J. Wen, N. M. Xiao, Z. F. Zhang, and M. L. Sui, J. Mater. Res. **23**, 2133 (2008).
[28] R. T. Qu, J. Eckert, and Z. F. Zhang, (unpublished).

[29]Z. F. Zhang and J. Eckert, Phys. Rev. Lett. **94**, 094301 (2005).
[30]R. T. Qu, F. F. Wu, Z. F. Zhang, and J. Eckert, J. Mater. Res. **24**, 3130 (2009).
[31]F. F. Wu, Z. F. Zhang, and S. X. Mao, Acta Mater. **57**, 257 (2009).
[32]P. E. Donovan and R. F. Cochrane, Scr. Metall. **22**, 1765 (1988).
[33]R. T. Qu *et al.* (unpublished).
[34]Y. Q. Cheng, A. J. Cao, H. W. Sheng, and E. Ma, Acta Mater. **56**, 5263 (2008).
[35]A. J. Cao, Y. Q. Cheng, and E. Ma, Acta Mater. **57**, 5146 (2009).
[36]F. Spaepen, Acta Metall. **25**, 407 (1977).
[37]A. S. Argon, Acta Metall. **27**, 47 (1979).
[38]P. S. Steif, F. Spaepen, and J. W. Hutchinson, Acta Metall. **30**, 447 (1982).
[39]D. Deng and B. Lu, Scr. Metall. **17**, 515 (1983).
[40]R. W. Cahn, N. A. Pratten, M. G. Scott, H. R. Sinning, and L. Leonardsson, *Studies of relaxation of metallic glasses by dilatometry and density measurements*, MRS Symposia Proceedings Vol. 28 (Materials Research Society, Pittsburgh, 1984), p. 241.
[41]A. S. Argon, J. Megusar, and N. J. Grant, Scr. Metall. **19**, 591 (1985).
[42]W. J. Wright, T. C. Hufnagel, and W. D. Nix, J. Appl. Phys. **93**, 1432 (2003).
[43]P. E. Donovan and W. M. Stobbs, Acta Metall. **29**, 1419 (1981).
[44]J. Li, Z. L. Wang, and T. C. Hufnagel, Phys. Rev. B **65**, 144201 (2002).
[45]W. H. Jiang and M. Atzmon, Acta Mater. **51**, 4095 (2003).
[46]F. F. Wu, Z. F. Zhang, F. Jiang, J. Sun, J. Shen, and S. X. Mao, Appl. Phys. Lett. **90**, 191909 (2007).
[47]H. S. Carslaw and J. C. Jaeger, *Conduction of Heat in Solids*, 2nd. (Clarendon, Oxford, 1986).
[48]K. M. Flores and R. H. Dauskardt, Acta Mater. **49**, 2527 (2001).
[49]Y. Liu, C. T. Liu, E. P. George, and X. Z. Wang, Appl. Phys. Lett. **89**, 051919 (2006).
[50]J. G. Wang, D. Q. Zhao, M. X. Pan, C. H. Shek, and W. H. Wang, Appl. Phys. Lett. **94**, 031904 (2009).